Nonlinear Analysis: Modelling and Control, 2009, Vol. 14, No. 4, 489–503

Transient Laminar MHD Free Convective Flow past a Vertical Cone with Non-Uniform Surface Heat Flux

Bapuji Pullepu[1], **A. J. Chamkha**[2]

[1]Department of Mathematics, Sathyabama University
Chennai, India-600119
bapujip@yahoo.com

[2]Manufacturing Engineering Department
The Public Authority for Applied Education and Training
Shuweikh, 70654 Kuwait
achamkha@yahoo.com

Received: 2009-02-04 **Revised:** 2009-09-04 **Published online:** 2009-11-11

Abstract. Numerical solution of unsteady laminar free convection from an incompressible viscous fluid flow past a vertical cone with non-uniform surface heat flux $q_w(x) = ax^m$ varying as a power function of the distance from the apex of the cone ($x = 0$) in the presence of a transverse magnetic field applied normal to the surface is considered. The dimensionless governing coupled partial differential boundary layer equations are formulated and solved numerically using an efficient and unconditionally stable finite-difference scheme of the Crank-Nicolson type. The numerical results are validated by comparisons with previously published work and are found to be in excellent agreement. The velocity and temperature fields have been studied for various combinations of physical parameters (Prandtl number Pr, exponent and magnetic parameter M). The local as well as the average skin-friction parameter and the Nusselt number are also presented and analyzed graphically.

Keywords: finite-difference method, free convection, MHD, non-uniform surface heat flux, vertical cone, unsteady flow.

a	constant
B_0	magnetic filed strength
$f''(0)$	local skin-friction in [16]
$f'(\eta)$	dimensionless velocity in X-direction in [16]
$F_0''(0)$	local skin friction in [20]
Gr_L	Grashof number
g	acceleration due to gravity
k	thermal conductivity
L	reference length
m	exponent in power law variation in surface heat flux
M	magnetic parameter
Nu_X	non-dimensional local Nuselt number
$\overline{NU}$	non-dimensional average Nuselt number
Pr	Prandtl number
q_w	rate of heat transfer per unit area
R	dimensionless local radius of the cone
r	local radius of the cone
T'	temperature
T	dimensionless temperature
t'	time
t	dimensionless time

U	dimensionless velocity in X-direction	X	dimensionless spatial co-ordinate along cone operator
u	velocity component in x-direction	x	spatial co-ordinate along cone generator
V	dimensionless velocity in Y-direction	Y	dimensionless spatial co-ordinate along the normal to the cone generator
v	velocity component in y-direction	y	spatial co-ordinate along the normal to cone generator

Greek symbols

α	thermal diffusivity	$1/\Phi_0(0)$	local Nusselt number in [20]
β	volumetric thermal expansion	μ	dynamic viscosity
η	dimensionless independent variable in [16]	ν	kinematic viscosity
ρ	density	τ_X	dimensionless local skin-friction parameter
σ	electrical conductivity of the fluid	$\overline{\tau}$	dimensionless average skin-friction parameter
ϕ	semi vertical angle of the cone	$-\theta(0)$	temperature in [16]

Subscripts

w	condition on the wall	∞	free stream condition

1 Introduction

Natural convection flows under the influence of a gravitational force have been investigated most extensively because they occur frequently in nature as well as in science and engineering applications. When a heated surface is in contact with the fluid, the result of temperature difference causes buoyancy force, which induces natural convection heat transfer. From a technological point of view, the study of convection heat transfer from a cone is of special interest and has wide range of practical applications. Mainly, these types of heat transfer problems deal with the design of spacecrafts, nuclear reactor, solar power collectors, power transformers, steam generators and others. Since 1953, many investigations [1–12] have developed similarity and non-similarity solutions for axi-symmetrical problems for natural convection flows over a vertical cone in steady state. Recently, Bapuji and Ekambavanan [13] have numerically studied the solutions of steady flows past plane and axi-symmetrical shape bodies. Also, Bapuji et al. [14, 15] have numerically studied the problem of transient natural convection from a vertical cone with isothermal and non-isothermal surface temperature using an implicit finite-difference method.

Recently heat flux applications are widely used in industries, engineering and science fields. Heat flux sensors can be used in industrial measurement and control systems. Examples of few applications are detection fouling (Boiler Fouling Sensor), monitoring of furnaces (Blast Furnace Monitoring/General Furnace Monitoring) and flare monitoring. Use of heat flux sensors can lead to improvements in efficiency, system safety and modeling. The studies [16–30] have considered problems of flow past a vertical cone/frustum of a cone in the case of uniform/non-uniform surface heat flux with porous/non-porous medium. Recently, Bapuji et al. [31] have numerically studied the problem of transient natural convection from a vertical cone with non-uniform surface heat flux using an implicit finite-difference method. All the above investigations [1–31] do not include deal with MHD effect.

MHD flow and heat transfer is of considerable interest because it can occur in many geothermal, geophysical, technological, and engineering applications such as nuclear reactors and others. The geothermal gases are electrically conducting and are affected by the presence of a magnetic field. Vajravelu and Nayfeh [32] studied hydromagnetic convection from a cone and a wedge with variable surface temperature and internal heat generation or absorption. Chamkha [33] considered the problem of steady-state laminar heat and mass transfer by natural convection boundary layer flow around a permeable truncated cone in the presence of magnetic field and thermal radiation effects, non-similar solutions were obtained and solved numerically by an implicit finite-difference methodology. Takhar et al. [34] developed the problem of unsteady mixed convection flow over a vertical cone rotating in an ambient fluid with a time-dependent angular velocity in the presence of a magnetic field. The coupled nonlinear partial differential equations governing the flow have been solved numerically using an implicit finite-difference scheme. Afify [35] studied the effects of radiation and chemical reaction on steady free convective flow and mass transfer of an optically dense viscous, incompressible and electrically conducting fluid past a vertical isothermal cone in the presence of a magnetic field. Afify's similarity equations were solved numerically using a fourth-order Runge-Kutta scheme with the shooting method. Later, Chamkha and Al-Mudhaf [36] focused on the study of unsteady heat and mass transfer by mixed convection flow over a vertical permeable cone rotating in an ambient fluid with a time-dependent angular velocity in the presence of a magnetic field and heat generation or absorption effects with the cone surface is maintained at variable temperature and concentration. Numerical solutions obtained, solving by the partial differential equations using an implicit, iterative finite-difference scheme. Recently, Elkabeir and Modather [37] studied chemical reaction, heat and mass transfer on MHD flow over a vertical isothermal cone surface in micropolar fluids with heat generation and absorption. Their numerical solutions were obtained by using the fourth-order Runge-Kutta method with shooting technique.

The present work is devoted to the study of transient laminar free convection flow past a vertical cone with non-uniform surface heat flux in the presence of a magnetic field. In order to check the accuracy of the numerical results, the present results are compared with the available results of Lin [16], Pop and Watanabe [17], Na and Chiou [23], Hossain and Paul [20] and are found to be in excellent agreement.

2 Mathematical analysis

The problem of axi-symmetrical, unsteady, laminar free convection flow of a viscous incompressible electrically-conducting fluid past a vertical cone with non-uniform surface heat flux under the influence of transversely applied magnetic field is formulated mathematically in this section. The following assumptions concerning the magnetic field and the geometry are made:

1. The magnetic field is constant and is applied in a direction perpendicular to the cone surface.
2. The magnetic Reynolds number is small so that the induced magnetic field is neglected and therefore, does not distort the magnetic field.
3. The coefficient of electrical conductivity is a constant throughout the fluid.
4. The Joule heating of the fluid (magnetic dissipation) and viscous dissipation are neglected.
5. The Hall effect of magnetohydrodynamics is neglected.
6. The system is considered as axi-symmetrical.
7. The effect of pressure gradient is assumed negligible.

The coordinate system is chosen (as shown in Fig. 1) such that x measures the distance along surface of the cone from the apex ($x = 0$) and y measures the distance normally outward.

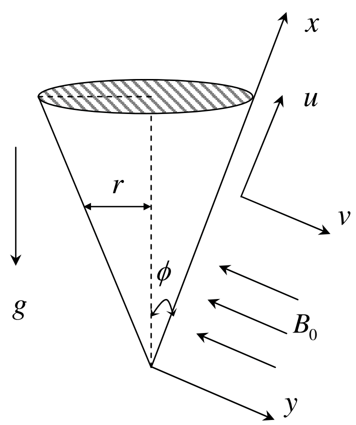

Fig. 1. Physical model and co-ordinate system.

Here, ϕ is the semi vertical angle of the cone and r is the local radius of the cone. Initially ($t' \leq 0$), it is also assumed that the cone surface and the surrounding fluid, which is at rest, have the same temperature T'_∞. Then at time $t' > 0$, it is assumed that heat is supplied from cone surface to the fluid at the rate $q_w(x) = ax^m$ and it is maintained at this value with m being a constant. The fluid properties are assumed constant except for density variations, which induce buoyancy force term in the momentum equation. The governing boundary layer equations of continuity, momentum and energy under Boussinesq approximation are as follows:

Equation of continuity

$$\frac{\partial}{\partial x}(ru) + \frac{\partial}{\partial y}(ru) = 0, \tag{1}$$

equation of momentum

$$\frac{\partial u}{\partial t} + u\frac{\partial u}{\partial x} + v\frac{\partial u}{\partial y} = g\beta\big(T' - T'_\infty\big)\cos\phi + \nu\frac{\partial^2 u}{\partial y^2} - \frac{\sigma B_0^2}{\rho}u, \tag{2}$$

equation of energy

$$\frac{\partial T'}{\partial t'} + u\frac{\partial T'}{\partial x} + v\frac{\partial T'}{\partial y} = \alpha\frac{\partial^2 T'}{\partial y^2}. \tag{3}$$

The initial and boundary conditions are

$$\begin{aligned} t' \le 0:\quad & u = 0,\quad v = 0,\quad T' = T'_\infty \quad \text{for all } x \text{ and } y,\\ t' > 0:\quad & u = 0,\quad v = 0,\quad \partial T'/\partial y = -q_w(x)/k \quad \text{at } y = 0,\\ & u = 0,\quad T' = T'_\infty \quad \text{at } x = 0,\\ & u \to 0,\quad T' \to T'_\infty \quad \text{as } y \to \infty. \end{aligned} \tag{4}$$

Further, we introduce the following non-dimensional variables:

$$\begin{aligned} & X = \frac{x}{L},\quad Y = \frac{y}{L},\quad t = \left(\frac{\nu}{L^2}Gr_L^{2/5}\right)t',\quad R = \frac{r}{L},\\ & U = \left(\frac{L}{\nu}\,Gr_L^{-2/5}\right)u,\quad V = \left(\frac{L}{\nu}\,Gr_L^{-1/5}\right)v,\\ & T = \frac{T' - T'_\infty}{L[q_w(L)/k]}\,Gr_L^{1/5},\quad M = \frac{\sigma B_0^2 L^2}{\mu}\,Gr^{-2/5}, \end{aligned} \tag{5}$$

where $Gr_L = g\beta[q_w(L)]L^4\cos\phi/\nu^2 k$ is the Grashof number based on L, $Pr = \nu/\alpha$ is the Prandtl number and $r = x\sin\phi$. Equations (1)–(3) can then be written in the following non-dimensional form:

$$\frac{\partial}{\partial X}(RU) + \frac{\partial}{\partial Y}(RV) = 0, \tag{6}$$

$$\frac{\partial U}{\partial t} + U\frac{\partial U}{\partial X} + V\frac{\partial U}{\partial Y} = T + \frac{\partial^2 U}{\partial Y^2} - MU, \tag{7}$$

$$\frac{\partial T}{\partial t} + U\frac{\partial T}{\partial X} + V\frac{\partial T}{\partial Y} = \frac{1}{Pr}\frac{\partial^2 T}{\partial Y^2}, \tag{8}$$

where M is the magnetic parameter.

The corresponding non-dimensional initial and boundary conditions are

$$\begin{aligned}
t \le 0&: \quad U = 0, \quad V = 0, \quad T = 0 \quad \text{for all } X \text{ and } Y,\\
t > 0&: \quad U = 0, \quad V = 0, \quad \partial T/\partial Y = -X^m \quad \text{at } Y = 0,\\
&\quad\ U = 0, \quad T = 0 \qquad \text{at } X = 0,\\
&\quad\ U \to 0, \quad T \to T'_\infty \quad \text{as } Y \to \infty.
\end{aligned} \tag{9}$$

Once the velocity and temperature profiles are known, it is interesting to study the local as well as the average skin-friction parameter and the rate of heat transfer at steady state and transient levels. The local non-dimensional skin-friction parameter τ_X and the local Nusselt number Nu_X are given by

$$\tau_X = Gr_L^{3/5}\left(\frac{\partial U}{\partial Y}\right)_{Y=0}, \quad Nu_X = \frac{X\,Gr_L^{1/5}}{T_{Y=0}}\left(-\frac{\partial T}{\partial Y}\right)_{Y=0}. \tag{10}$$

Also, the non-dimensional average skin-friction parameter $\overline{\tau}$ and the average Nusselt number $\overline{Nu}$ can be written as

$$\overline{\tau} = 2Gr_L^{3/5}\int_0^1 X\left(\frac{\partial U}{\partial Y}\right)_{Y=0}\mathrm{d}X, \quad \overline{Nu} = 2Gr_L^{1/5}\int_0^1 \frac{X}{T_{Y=0}}\left(-\frac{\partial T}{\partial Y}\right)_{Y=0}\mathrm{d}X. \tag{11}$$

The derivatives involved in equations (10) and (11) are obtained using five-point approximation formula and then the integrals are evaluated using Newton-Cotes closed integration formula.

3 Solution procedure

The governing partial differential equations (6)–(8) are unsteady, coupled and non-linear with initial and derivative boundary conditions (9). They are solved numerically by an implicit finite-difference method of Crank-Nicolson type as described in detail by Bapuji et al. [14, 15]. The region of integration is considered as a rectangle with sides $X_{max} = 1.0$ and $Y_{max} = 26$, where Y_{max} corresponds to $Y = \infty$ which lies very well outside the momentum and thermal boundary layers. The finite-difference scheme is unconditionally stable as explained by Bapuji et al. [15]. Stability and compatibility ensure the convergence.

4 Results and discussion

In order to prove the accuracy of our numerical results, the present results for the steady-state flow conditions at $X = 1.0$ when $M = 0$ (i.e. the absence of magnetic field effect) are compared with available solutions from the open literature. The velocity and temperature profiles of the cone for $Pr = 0.72$ are displayed in Fig. 2 and the numerical values of local skin-friction τ_X and temperature T for different values of Prandtl number are shown in Table 1 and are compared with similarity solutions of Lin [16] in steady state using suitable transformation ($Y = (20/9)^{1/5}\eta$, $T = (20/9)^{1/5}(-\theta(0))$, $U = (20/9)^{3/5}f'(\eta)$, $\tau_X = (20/9)^{2/5}f''(0)$). In addition, the local skin-friction τ_X and the local Nusselt number Nu_X for different values of Prandtl number when heat flux gradient power $m = 0.5$ at $X = 1.0$ in steady state are compared with the non-similarity results of Hossain and Paul [20] in Table 2. It is observed that the results are in good agreement with each other. It is also noticed that the present results agree well with those of Pop and Watanabe [17], Na and Chiou [23] (as pointed out in Table. 1).

Table 1. Comparison of steady state local skin-friction parameter and temperature values at X=1.0 with those of Lin [16]

$M = 0$	Temperature			Local skin friction		
	Lin results [16]		Present results	Lin results [16]		Present results
Pr	$-\theta(0)$	$-(\frac{20}{9})^{1/5}\theta(0)$	T	$f''(0)$	$(\frac{20}{9})^{1/5}f''(0)$	τ_X
0.72	1.52278 1.52278[a]	1.7864	1.7796	0.88930 0.88930[a]	1.224	1.2154
1	1.39174	1.6327 1.6329[b]	1.6263	0.78446	1.0797	1.0721
2	1.16209	1.3633	1.3578	0.60252	0.8293	0.8235
4	0.98095	1.1508	1.1463	0.46307	0.6373	0.6328
6	0.89195	1.0464	1.0421	0.39688	0.5462	0.5423
8	0.83497	0.9796	0.9754	0.35563	0.4895	0.4859
10	0.79388	0.9314	0.9272	0.32655	0.4494	0.4460
100	0.48372	0.5675	0.5604	0.13371	0.184	0.1813

[a] Values taken from Pop and Watanabe [17] when suction/injection is zero.
[b] Values taken from Na and Chiou [23] when and solutions for flow over a full cone.

Table 2. Comparison of steady-state local skin-friction parameter and local Nusselt number values at $X = 1.0$ with those of Hossain and Paul [20] for different values of Pr when $m = 0.5$ and suction is zero

$M = 0$	Local skin-friction		Local Nusselt number	
	Hossain results [20]	Present results	Hossain results [20]	Present results
Pr	$F''(0)$	$\tau_X/(Gr_L)^{3/5}$	$1/\Phi_0(0)$	$Nu_X/(Gr_L)^{1/5}$
0.01	5.13457	5.1155	0.14633	0.1458
0.05	2.93993	2.9297	0.26212	0.2630
0.1	2.29051	2.2838	0.33174	0.3324

Figures 3 through 6 present transient velocity and temperature profiles at $X = 1.0$ for various parameters Pr, m and magnetic parameter M. The value of t with star ($*$) symbol denotes the time taken to reach steady state. In Figs. 3 and 4, transient velocity and temperature profiles are plotted for various values of Pr and M. Application of a magnetic field normal to the flow of an electrically conducting fluid gives rise to a resistive force that acts in the direction opposite to that of the flow. This force is called the Lorentz force. This resistive force tends to slow down the motion of the fluid along the cone and causes an increase in its temperature and a decrease in velocity as M increases. This is clear from Figs. 3 and 4. Also, it is observed from these figures that the momentum and thermal boundary layers become thick when the values of Pr decrease or the values of M increase. The viscous force increases and thermal diffusivity reduces with increasing values of Pr, causing a reduction in the velocity and temperature. It is also noticed that the time taken to reach steady-state conditions increases with increasing values of Pr or M. It is noticed from the Figs. 3 and 4 that the temporal maximum value of velocity reaches steady state only when the value of increases and that there is insignificant effect on the temperature profiles.

In Figs. 5 and 6, transient velocity and temperature profiles are plotted for various values of m with $M = 1.0$ and $Pr = 0.71$. Impulsive forces are reduced along the surface of the cone near the apex for increasing values of m (i.e. the gradient of heat flux along the cone near the apex reduces with increasing values of m). Due to this, the difference between temporal maximum velocity values and steady-state values reduces with increasing values of m and that there is no significant effect on temperature profiles as noticed from Fig. 6. It is also observed that increasing m reduces the velocity as well as the temperature and takes more time to reach steady-state conditions.

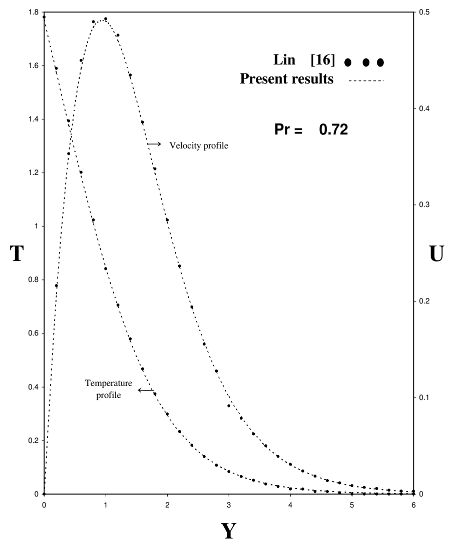

Fig. 2. Comparison of steady state temperature and velocity profiles at X=1.0.

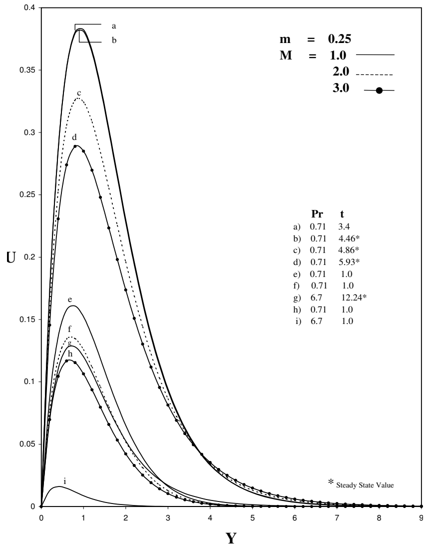

Fig. 3. Transient velocity profiles at X=1.0 for various values of Pr and M.

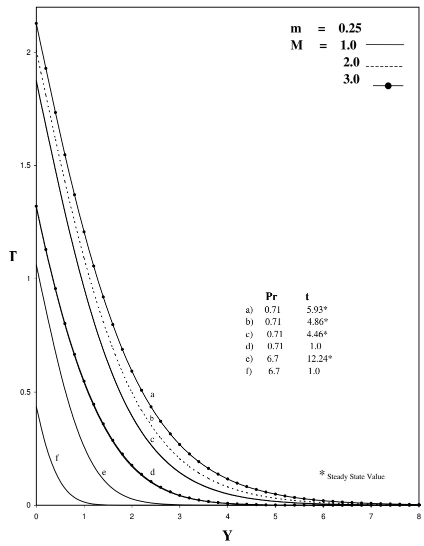

Fig. 4. Transient temperature profiles at X=1.0 for various values of Pr and M.

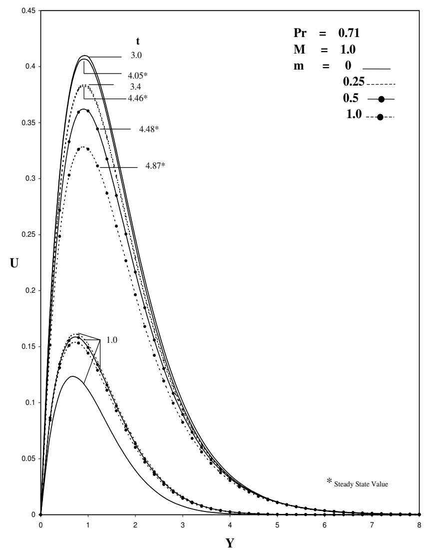

Fig. 5. Transient velocity profiles at X=1.0 for various values of m.

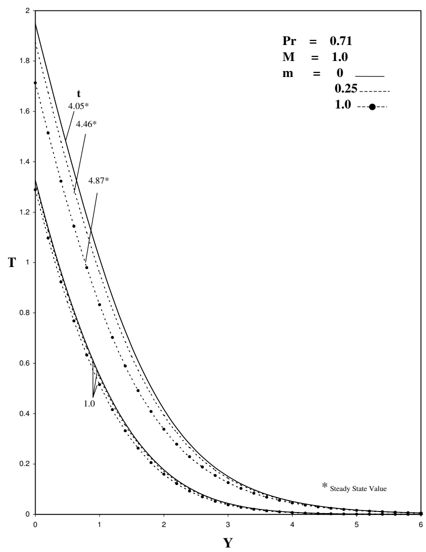

Fig. 6. Transient temperature profiles at X=1.0 for various values of m.

Figures 7 through 10 depict the variations of the transient local skin-friction parameter τ_X and the local Nusselt number Nu_X at various positions on the surface of the cone ($X = 0.25$ and 1.0) for controlling parameters m, Pr and M. The local skin-friction parameter τ_X and the local Nusselt number Nu_X for different values of Pr and M at various positions on the surface of the cone ($X = 0.25$ and 1.0) in the transient period are shown in Figs. 7 and 8, respectively. It is observed that the local skin-friction parameter and the local Nusselt number decreases with increasing values of M and the effect of M on the local skin-friction parameter τ_X and the local Nusselt number Nu_X is less near the apex of the cone and increases gradually with increasing the distance along the surface of the cone from the apex. Also, it is noticed from Fig. 7 that the local wall shear stress decreases as Pr increases because the velocity decreases with an increasing value of Pr as shown in Fig. 3. The local Nusselt number Nu_X increases with increasing values of Pr and this is clear from Fig. 8. The variation of the local skin-friction parameter τ_X and the local Nusselt number Nu_X in the transient period at various positions on the surface of the cone ($X = 0.25$ and 1.0) and for different values of m are shown in Figs. 9 and 10. It is observed from Fig. 9 that the local skin-friction parameter decreases with increasing values of m and that the effect of m on the local skin-friction τ_X is more near the apex of the cone and reduces gradually with increasing the distance along the surface of the cone from the apex. From Fig. 10, it is noticed that near the apex, the local Nusselt number Nu_X reduces with increasing values of but this trend is slowly changed and reversed as the distance increases along the surface from apex.

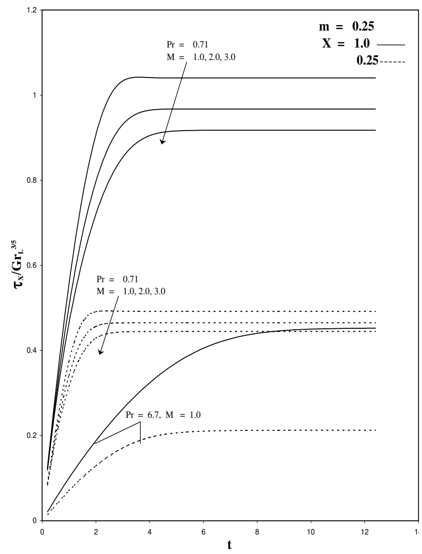

Fig. 7. Local skin friction at $X = 0.25$ and 1.0 for various values of Pr and M in transient period.

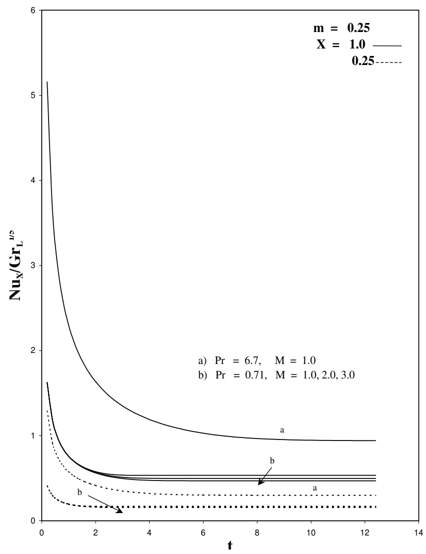

Fig. 8. Local Nusselt number at $X = 0.25$ and 1.0 for various values of Pr and M in transient period.

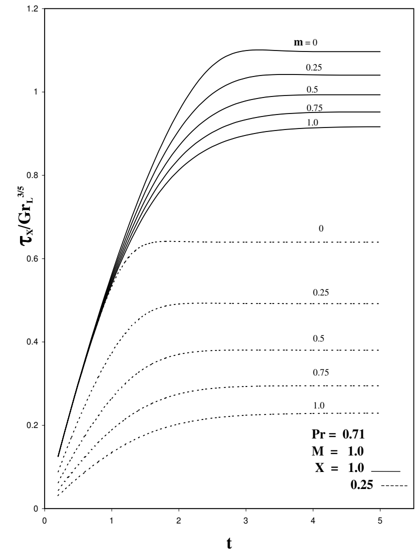

Fig. 9. Local skin friction at $X = 0.25$ and 1.0 for various values of m in transient period.

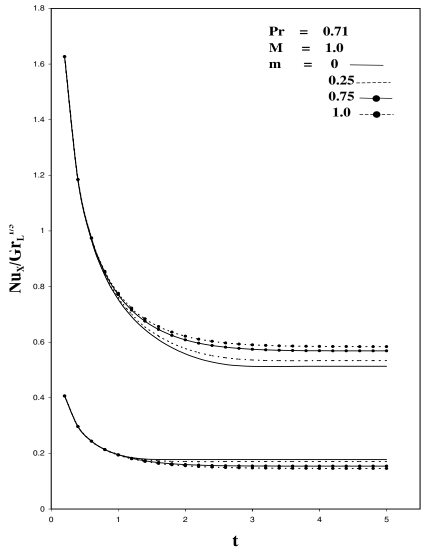

Fig. 10. Local Nusselt number at $X = 0.25$ and 1.0 for various values of m in transient period.

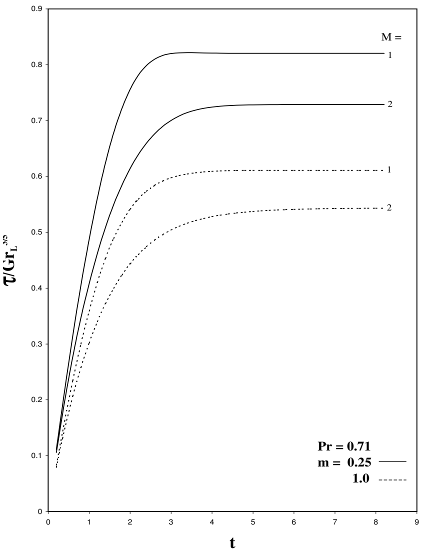

Fig. 11. Average skin friction for various values of m and M.

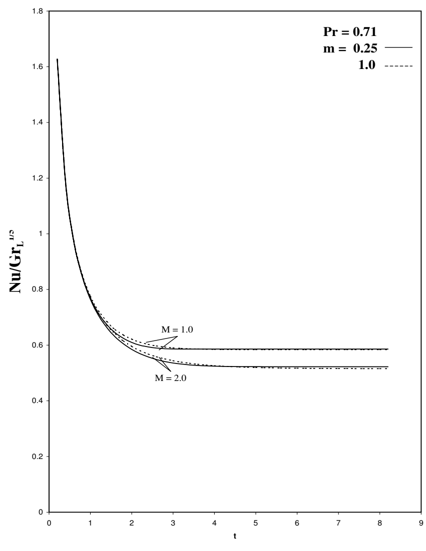

Fig. 12. Average Nusselt number for various values of m and M.

Finally, Figs. 11 and 12 illustrate the effects of m and M on the average skin-friction parameter $\overline{\tau}$ and the average Nusselt number $\overline{Nu}$ in the transient period. The average skin-friction parameter $\overline{\tau}$ is more for lower values of m. It is observed from Figs. 11 and 12 that the values of the average skin-friction parameter $\overline{\tau}$ and the average Nusselt number $\overline{Nu}$ decrease with increasing values of M. In addition, it is clear from the Fig. 12, the effect of m is almost negligible on the average Nusselt number $\overline{Nu}$.

5 Conclusions

This paper deals with unsteady laminar free convection flow of an electrically-conducting fluid past a vertical cone with non-uniform surface heat flux in the presence of a transverse magnetic field. The dimensionless governing boundary-layer equations are solved numerically using an implicit finite-difference method of the Crank-Nicolson type. Present results are compared with available results from the open literature and found to be in very good agreement. The following conclusions are drawn:

- The time taken to reach steady state increases with increasing values of Pr, m and M.
- The velocity U increases when the controlling parameters Pr, m and M are reduced.
- The surface temperature T reduces as the values of M decrease and the values of Pr, m increase.
- The momentum and thermal boundary layers become thick for lower values of Pr or higher values of M.
- The values of the local skin-friction parameter τ_X and the local Nusselt number Nu_X reduce as M increases.
- The local skin-friction parameter τ_X decreases while the local Nusselt number Nu_X increases with increasing values of Pr.
- The local and average skin-friction parameters increase when the value of m is reduced.
- The average skin-friction parameter and the average Nusselt number reduce when the values of M increases.
- The effect of m on the average Nusselt number $\overline{Nu}$ is almost negligible.

References

1. H. J. Merk, J. A. Prins, Thermal convection laminar boundary layer, I, II, *Appl. Sci. Res. A4*, **11**(24), pp. 195-206, 1953, 1954.

2. R. G. Hering, R. J. Grosh, Laminar free convection from a non-isothermal cone, *Int. J. Heat Mass Tran.*, **5**, pp. 1059–1068, 1962.
3. R. G. Hering, Laminar free convection from a non-isothermal cone at low Prandtl number, *Int. J. Heat Mass Tran.*, **8**, pp. 1333–1337, 1965.
4. S. Roy, Free convection from a vertical cone at high Prandtl numbers, *Trans. ASME Journal of Heat Transfer*, **96**, pp. 115–117, 1974.
5. R. S. R. Gorla, R. A. Startman, Natural convection boundary layer flow of water at $4\,^{\circ}$C past slender cones, *Int. Commun. Heat Mass*, **13**, pp. 403–411, 1986.
6. M. Alamgir, Overall heat transfer from vertical cones in laminar free convection: an approximate method, *ASME J. Heat Transf.*, **101**, pp. 174–176, 1989.
7. I. Pop, H. S. Takhar, Compressibility effects in laminar free convection from a vertical cone, *Appl. Sci. Res.*, **48**, pp. 71–82, 1991.
8. G. Ramanaiah, V. Kumaran, Natural convection about a permeable cone and a cylinder subjected to radiation boundary condition, *Int. J. Engg Sci.*, **30**, pp. 693–699, 1992.
9. M. A. Hossain, S. C. Paul, Free convection from a vertical permeable circular cone with non-uniform surface temperature, *Acta Mech.*, **151**, pp. 103–114, 2001.
10. I. Pop, T. Grosan, M. Kumari, Mixed convection along a vertical cone for fluids of any Prandtl number case of constant wall temperature, *Int. J. Numer. Method. H.*, **13**, pp. 815–829, 2003.
11. H. S. Takhar, A. J. Chamkha, G. Nath, Effect of thermo-physical quantities on the natural convection flow of gases over a vertical cone, *Int. J. Eng. Sci.*, **42**, pp. 243-256, 2004.
12. Md. M. Alam, M. A. Alim, Md. M. K. Chowdhury, Free convection from a vertical permeable circular cone with pressure work and non-uniform surface temperature, *Nonlinear Anal. Model. Control*, **12**(1), pp. 21–32, 2007.
13. Bapuji Pullepu, K. Ekambavanan, Natural convection effects on two dimensional axi-symmetrical shape bodies (flow past a vertical/cone/thin cylinder) and plane shape bodies (flow over a vertical/ inclined/ horizontal plates), in: *Proceedings of 33rd National and 3rd International Conference on Fluid Mechanics and Fluid Power, December 7–9, IIT, Bombay, India*, paper No. 1707, 2006.
14. Bapuji Pullepu, K. Ekambavanan, Ali J. Chamkha, Unsteady laminar natural convection flow past an isothermal vertical cone, *Int. J. Heat Technology*, **25**(2), pp. 17–28, 2007.
15. Bapuji Pullepu, K. Ekambavanan, I. Pop, Finite difference analysis of laminar free convection flow past a non isothermal vertical cone, *Heat Mass Transfer*, **44**, pp. 517–526, 2008.
16. F. N. Lin, Laminar convection from a vertical cone with uniform surface heat flux, *Lett. Heat Mass Trans.*, **3**, pp. 49–58, 1976.
17. I. Pop, T. Watanabe, Free convection with uniform suction or injection from a vertical cone for constant wall heat flux, *Int. Commum. Heat Mass*, **19**, pp. 275–283, 1992.
18. M. Hasan, A. S. Mujumdar, Coupled heat and mass transfer in natural convection under flux condition along a vertical cone, *Int. Commun. Heat Mass*, **11**, pp. 157–172, 1984.

19. M. Kumari, I. Pop, Free convection over a vertical rotating cone with constant wall heat flux, *Journal of Applied Mechanics and Engineering*, **3**, pp. 451–464, 1998.

20. M. A. Hossain, S. C. Paul, Free convection from a vertical permeable circular cone with non-uniform surface heat flux, *Heat Mass Transfer*, **37**, pp. 167–173, 2001.

21. M. A. Hossain, S. C. Paul, A. C. Mandal, Natural convection flow along a vertical circular cone with uniform surface temperature and surface heat flux in a thermally stratified medium, *Int. J. Numer. Method. H.*, **12**, pp. 290–305, 2002.

22. T. Y. Na, J. P. Chiou, Laminar natural convection over a slender vertical frustum of a cone, *Wärme-ünd Stoffübertragung*, **12**, pp. 83–87, 1979.

23. T. Y. Na, J. P. Chiou, Laminar natural convection over a frustum of a cone, *Appl. Sci. Res.*, **35**, pp. 409–421, 1979.

24. T. Y. Na, J. P. Chiou, Laminar natural convection over a slender vertical frustum of a cone with constant wall heat flux, *Wärme-ünd Stoffübertragung*, **13**, pp. 73–78, 1980.

25. R. S. R. Gorla, V. Krishnan, I. Pop, Natural convection flow of a power-law fluid over a vertical frustum of a cone under uniform heat flux conditions, *Mech. Res. Commun.*, **21**, pp. 139–146, 1994.

26. I. Pop, T. Y. Na, Natural convection over a vertical wavy frustum of a cone, *Int. J. Nonlinear Mech.*, **34**, pp. 925–934, 1999.

27. T. Y. Wang, C. Kleinstreuer, Thermal convection of micro polar fluids past two dimensional or axisymmetric bodies with suction injection, *Int. J. Eng. Sci.*, **26**, pp. 1261–1277, 1988.

28. K. A. Yih, Uniform transpiration effect on combined heat and mass transfer by natural convection over a cone in saturated porous media: uniform wall temperature/concentration or heat/mass flux, *Int. J. Heat Mass Tran.*, **42**, pp. 3533–3537, 1999.

29. K. A. Yih, Coupled heat and mass transfer by free convection over a truncated cone in porous media: VWT/VWC or VHF/VMF, *Acta Mech.*, **137**, pp. 83–97, 1999.

30. T. Grosan, A. Postelnicu, I. Pop, Free convection boundary layer over a vertical cone in a non newtonian fluid saturated porous medium with internal heat generation, *Technische Mechanik Band*, **24**(4), pp. 91–104, 2004.

31. Bapuji Pullepu, K. Ekambavanan, I. Pop, Transient laminar free convection from a vertical cone with non-uniform surface heat flux, *Studia Univ. Babes-Bolyai Mathematica*, **LIII**(1), pp. 75–99, 2007.

32. K. Vajravelu, L. Nayfeh, Hydromagnetic convection at a cone and a wedge, *Int. Commun. Heat Mass*, **19**, pp. 701–710, 1992.

33. A. J. Chamkha, Coupled heat and mass transfer by natural convection about a truncated cone in the presence of magnetic field and radiation effects, *Numer. Heat Transfer*, **39**, pp. 511–530, 2001.

34. H. S. Takhar, A. J. Chamkha, G. Nath, Unsteady mixed convection flow from a rotating vertical cone with a magnetic field, *Heat Mass Transfer*, **39**, pp. 297–304, 2003.

35. A. A. Afify, The effect of radiation on free convective flow and mass transfer past a vertical isothermal cone surface with chemical reaction in presence of transverse magnetic field, *Can. J. Phys.*, **82**, pp. 447–458, 2004.

36. A. J. Chamkha, A. Al-Mudhaf, Unsteady heat and mass transfer from a rotating vertical cone with a magnetic field and heat generation or absorption effects, *Int. J. Therm. Sci.*, **44**, pp. 267–276, 2005.

37. S. M. M. EL-Kabeir, M. Modather, M. Abdou, Chemical reaction heat and mass transfer on MHD flow over a vertical isothermal cone surface in micropolar fluids with heat generation/absorption, *Applied Mathematical Sciences*, **1**(34), pp. 1663–1674, 2007.